2017

Baseline Rolling Resistance for Tires' On-Road Fuel Efficiency Using Finite Element Modeling

Jaime Hernandez
Marquette University, jaime.hernandez@marquette.edu

Imad L. Al-Qadi
University of Illinois - Urbana-Champaign

Hasan Ozer
University of Illinois at Urbana-Champaign

International Journal of Pavement Engineering, Vol. 18, No. 5 (2017): 424-432. DOI.

Baseline rolling resistance for tires' on-road fuel efficiency using finite element modeling

Jaime A. Hernandez
Department of Civil and Environmental Engineering, University of Illinois at Urbana-Champaign, Urbana, IL, USA.
Imad L. Al-Qadi
Department of Civil and Environmental Engineering, University of Illinois at Urbana-Champaign, Urbana, IL, USA.
Hasan Ozer
Department of Civil and Environmental Engineering, University of Illinois at Urbana-Champaign, Urbana, IL, USA.

Abstract

Calculation of truck tires rolling resistance, using the finite element method and considering variables such as incompressible visco-hyperelastic rubber materials, accurate tire geometry and steady temperature distribution, is presented. The model was validated using experimentally measured contact area and contact stresses. Rolling resistance was calculated for three values of axle load, tire

inflation pressure, temperature and speed. In addition, regression analysis was used to propose a mathematical expression for predicting rolling resistance as a function of the considered variables. Finally, the contribution of tire's rubber components to the internal energy was quantified, and it was found that sidewall and subtread were the most relevant. The results of this study will help differentiate the contribution of pavement parameters, such as mean profile depth and international roughness index, to fuel efficiency.

Keywords:

Rolling resistance, fuel efficiency, tire modelling, energy loss, coefficient of rolling resistance

1. Introduction

As part of the Climate Action Plan for the United States, higher fuel efficiency standards will be established for all highway vehicles, including passenger cars and heavy trucks. These standards aim at reducing greenhouse gas (GHG) emissions associated with the transportation sector. Transportation services consume nearly 28% of total energy use in the US and a big share is in the form of petroleum. Even more, the American government announced in June 2015 a plan to reduce truck emissions. The transportation sector is a significant source of GHG emissions, accounting for 39% of total US GHG emissions in 2011. Hence, efforts by the transportation industry, including highway and trucking industry, are currently focused on enhancing sustainability practices, such as reducing fuel consumption, sustainable infrastructure materials, roadside elements, construction and operations (Bureau of Transportation Statistics 2013). For example, the regulations imposed by the Environmental Protection Agency limit various sources of emissions for on-road and non-road vehicles and engines.

For semi-trucks fabricated from 2018, a 20% reduction in fuel consumption will be required (The White House 2014). Such targets can be achieved by improving engine technology, using alternative fuels, upgrading and maintaining old vehicles, and vehicle and tire design. Therefore, it is important to understand vehicles fuel consumption mechanisms to be able to achieve such goals.

The energy provided by fuel is used to overcome five resistive forces when the vehicle is moving: rolling resistance, drag forces, internal friction in the vehicle, gravitational forces and inertial forces (Michelin of Americas 2003). Tires greatly affect vehicles rolling resistance forces, thus contributing to energy consumption. Rolling resistance is directly related to vehicles tires, and its contribution to fuel consumption has been quantified for various scenarios. For instance, Schuring and Redfield (1982) assumed a linear relationship between rolling resistance and fuel consumption and observed a variation in energy loss ranging between 7 and 17%, depending on tire type and load. The linear relation between rolling resistance and vehicle fuel consumption was verified and updated by Schuring (1994).

In addition, road surface characteristics play a role in the rolling resistance of tires. Mammetti *et al.* (2013) reported 25–30% contribution of rolling resistance to fuel consumption depending on the road type (city, rural, or highway). Laclair and Russell (2005) observed savings of 4.77 lt/100 km on secondary roads and 5.49 lt/100 km on highway per 1-kN reduction on rolling resistance. The finding was based on measurements of a truck's fuel consumption, rolling resistance of tires and validated modelling using the commercial software AVL-CRUISE. In general, fuel consumption and vehicle wear

and tear are correlated to road surface smoothness. According to Chatti and Zaabar (2012), a unit increase of roughness will increase fuel consumption of passenger cars by about 2% and about 1% for heavy trucks, respectively. A linear relationship was established to indicate the correlation between road roughness and additional fuel consumption for different classes of vehicles.

To understand the factors influencing the rolling resistance of tires and develop simplified predictive models, mathematical expressions have been proposed in the literature to predict rolling resistance based on experimental evidence and field observations. For example, Clark (1978) assumed rolling resistance as a linear combination of applied load and the inverse of tire inflation pressure. The obtained expression characterised a specific tire and needed three experimental measurements to be fully defined. Grover proposed the equation for rolling resistance currently used by Standard SAE J2452. The formula considered load, tire inflation pressure and speed. Although the formula provided very good fit, it did not consider temperature (Grover 1998). This drawback was addressed by Nielsen and Sandberg (2002) who proposed an analytical procedure that consists of five equations based on the individual effects of the variables considered on rolling resistance coefficient. The procedure accounted for temperature, velocity and load and provided good agreement with published results. SAE J2452 expression is adjusted in this paper to include temperature effects without any system of equations.

Finite element (FE) is another powerful tool used to predict rolling resistance. Even though the method considers advanced features, such as tire-surface contact, incompressible visco-hyperelastic materials and large deformations, it requires considerable computational resources. Simplified approaches have been adopted, thus affecting accuracy of the results. Shida *et al.* (1999) estimated rolling resistance based on static analysis of the tire and laboratory-determined viscoelastic properties of tire materials. The method was successful in capturing the trend of the considered variables. Ebbott *et al.* (1999) used a simplified thermomechanical approach to compute rolling resistance and steady temperature distribution.

Some issues were observed when comparing FE simulation results with experimental measurements because of the frictionless contact assumptions. Terziyski and Kennedy used FE to calculate rolling resistance and steady temperature distribution of passenger cars. The approach utilised a statically loaded tire model with linear elastic rubber with Poisson's ratio of 0.48. Coulomb friction was assumed between the tire and the surface with a coefficient of 0.75. The hysteresis was obtained by post-processing of the finite results. Measured and predicted rolling resistance differed by more than 30%, which could be the result of the inappropriate material model (Terziyski and Kennedy 2009).

Tires rolling resistance is an important component of vehicles driving resistance. Therefore, it is important to understand the mechanisms of tires rolling resistance and tires interaction with the environment and road surface to improve accuracy of rolling resistance prediction models, especially with the emergence of new tire designs that focus on reducing fuel consumption, such as the new-generation wide-base tires (Muster 2000, GENIVAR 2005, Ang-Olson and Schroeer 2002, Nylund 2006, Franzese *et al.* 2010). Therefore, the objective of this paper is to develop a rolling resistance model for a truck tire based on numerical simulations, capturing the complexity of tire design and operating conditions and its interaction with the environment. This paper presents a baseline rolling resistance predictive model for a truck tire developed using 3-D FE simulations. The ultimate objective of the

study is to expand the baseline model to capture the contribution of road structure and surface conditions.

In this paper, a brief background on rolling resistance is presented. Details of tire FE model are explained. The numerical analysis matrix is introduced to evaluate the effect of temperature, speed, load and tire inflation pressure on rolling resistance. Two approaches for calculating rolling resistance are discussed: the first is based on the energy dissipated by the tire while the second is based on the horizontal reaction force at the tire-pavement interface during free rolling. A numerical expression for predicting the baseline rolling resistance of the analysed tire is also presented. Finally, the contribution of viscoelastic rubber components to the internal energy is given.

2. Rolling resistance definition

Rolling resistance is defined as the energy dissipated by the tire per unit distance travelled. The sources of energy dissipation in the tire are the hysteresis of the material used for tire fabrication, the friction between tire and pavement, and the friction between tire and air. However, hysteresis has been the main focus of research because it represents 90–95% of rolling resistance (Walter and Conant 1974, Clark 1978, Michelin of Americas 2003). When subjected to one loading cycle, the path followed by the stress-strain curve is not the same when loading as when unloading. As a consequence, the strain energy when the load is applied is not equal to the strain energy when the load is removed. This behaviour helps define total energy, dissipated energy and recovered energy as the area under the loading path, between loading and unloading path, and under unloading path, respectively. Some studies have identified a close relation between rolling resistance and loss ratio (ratio between energy dissipated and energy input) and loss tangent (tangent of phase angle) for the same tire structure (Lou 1978). Rolling resistance from material energy dissipation is identified as RR_e.

A mechanical manifestation of rolling resistance is a horizontal force developed at the contact between tire and road surface during free rolling (RR_f). Some studies have experimentally proved this link. For instance, Pillai compared the rolling resistance from hysteresis and horizontal reaction methods for car tires without treads and found good agreement (Pillai 1995). It has been observed that RR_f is directly proportional to the applied load P; the ratio between RR_f and P is known as coefficient of rolling resistance C_{rr}. Under specific assumptions, an energy balance was used to prove that C_{rr} depends only on the loss ratio if the term $\delta b/A_c$ is constant, where δ is the tire deflection, b is the contact width and A_c is the contact area (Pillai and Fielding-Russell 1992).

Two approaches for measuring rolling resistance are standardised by the Society of Automotive Engineers (SAE) under SAE J1269 and SAE J2452 (Society of Automotive Engineers 2006, Society of Automotive Engineers 1999). SAE J1269 procedure provides the steady rolling resistance tires for passenger cars, light trucks, heavy trucks and buses. The test is performed under constant speed and steady temperature (24°C) with the tire subjected to four combinations of load and inflation pressure. The loading conditions depend on the maximum load of the tire and its base tire inflation pressure (Society of Automotive Engineers 2006). On the other hand, SAE J2452 aims to represent the coastdown operation of vehicles and is based on four combinations of load and tire inflation pressure, which are defined by the maximum tire load and tire inflation pressure. For each combination, the speed varies as a function of time between 15 and 115 km/h (Society of Automotive Engineers 1999).

Wen et al. compared SAE J1269 and SAE J2452 for passenger car tires and found good correlation between both procedures based on statistical analysis (Wen *et al.* 2014). FE simulations were used in this study to calculate rolling resistance.

3. Tire FE model

A wide-base tire with a width of 445 mm and properly measured geometric details was modelled using the FE method. The geometric details included distribution of materials in the cross section and tread and groove thicknesses. The tire was assumed to be made of five rubber elements (tread, sub-tread, shoulder wedge, sidewall and bead filler) and five reinforcement belts. The width, orientation, spacing and cross-sectional area were measured for each belt. The distribution of rubber components in the half cross section is presented in Figure 1.

Figure 1. Distribution of material properties in tire's half cross section.

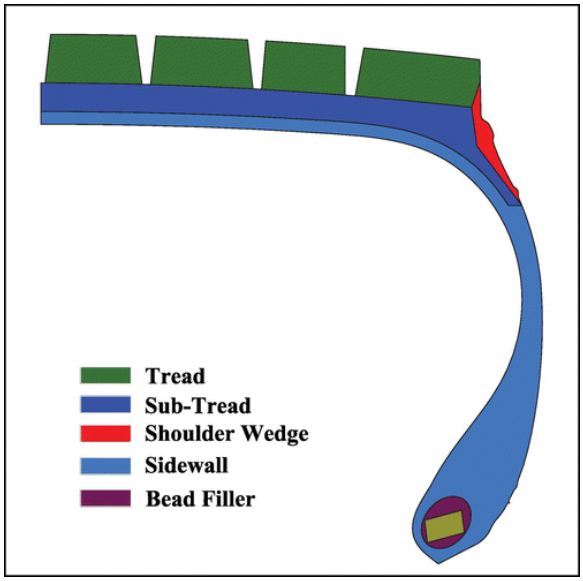

The modelled tire was previously used in an experimental programme aimed to measure contact area and contact stresses (Hernandez *et al.* 2013). The measurements were used to calibrate and validate the developed FE model. The results obtained from a specific combination of load and tire inflation pressure influenced the change of Mooney-Rivlin constants. After that, another eight combinations of load and tire inflation pressure were used to validate the model. The mean average percentage error for contact area and deflection was 4.2 and 8.5%, respectively Hernandez and Al-Qadi 2015.

3.1. Constitutive models

Appropriate material models were used for the various tire components. Rubber was assumed to behave as visco-hyperelastic material with long-term behaviour as defined by Mooney-Rivlin model. Viscoelastic parameters in the form of Prony series were obtained from dynamic mechanic analyser (DMA) tests conducted at different temperatures and frequency. The hyperelasticity component of the rubber constitutive relationship considers the large deformation behaviour under high truck loads and tire inflation pressures, whereas the viscoelastic component represents energy losses in the rubber as a result of load-unload cycles. Figure 2(a) presents a sample of the DMA test results for a rubber component. Prony series calculations and testing temperature errors are also shown. In addition, belts

were assumed linear elastic with experimentally obtained elastic modulus. Figure 2(b) shows a test result sample for tension testing of the belts. The plot includes the results of five specimens along with the average elastic modulus represented by the slope of the linear segment. Finally, for the rolling tire, the Coulomb friction with $\mu = 0.30$ was assumed at the interface between the tire and the pavement.

Figure 2. Sample of material testing and characterisation: (a) viscoelastic rubber, (b) elastic belt.

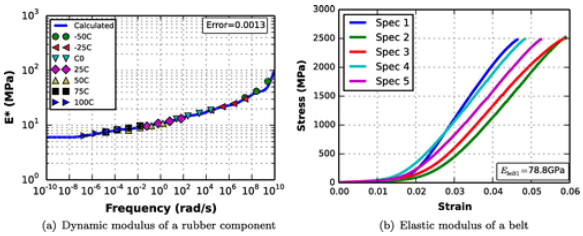

(a) Dynamic modulus of a rubber component (b) Elastic modulus of a belt

3.2. FE mesh and analysis

Various element types were used to properly model the complexity of the tire structure. The tire volume was divided into two regions: The foot, which is the region in potential contact with the ground, covered a 60°-arc and was symmetric with respect to the vertical axis; and the cylindrical elements, which exactly represent the curved geometries, were used in the rest of the tire circumference (Danielson and Noor 1997, Kennedy 2003). Full integration elements were utilised in the first region. Figure 3 shows both regions with a 3-D and side view of the tire model. In order to properly account for incompressibility, hybrid elements were assigned in the regions occupied by rubber. Finally, reinforcement was modelled using rebar elements, which consider each component, rubber and reinforcement, independently (Helnwein *et al.* 1993).

Figure 3. 3D and side view of tire's FE model.

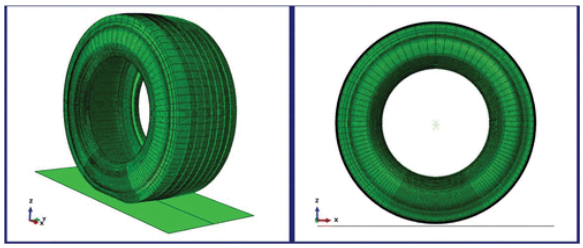

A convergence analysis based on the strain energy criterion was conducted to determine the size of the cylindrical elements used in the mesh, including cross section and foot. Therefore, strain energy was calculated for each mesh generated with various element sizes. The reference solution was chosen to be the mesh with the finest element size. Optimum mesh had strain energy within 5% the value of the reference solution. This procedure was applied to the half-axisymmetric model to determine the size of elements in the cross section and to the half model to define the size of cylindrical elements and the elements in the foot region. The mesh sensitivity analysis was performed assuming hyperelastic rubber materials. The final mesh consisted of 60 full integration elements in the foot region (i.e. each element covered 1°), and 40 cylindrical elements at each side of the foot.

The steady-state transport feature of Abaqus was used to perform the calculation. This approach is based on the arbitrary Lagrangian Eulerian (ALE) formulation, which combines the advantages of the Lagrangian and Eulerian methods. In the case of rolling tire, the reference coordinate system is located at the tire rotation axis, and the mapping between the initial and reference configuration is a pure rigid

body motion. The ALE approach transforms a dynamic problem into one with spatial derivative and allows for the use of finer mesh at the tire-surface contact only.

The analysis was performed in three successive stages: (i) axisymmetric tire model was loaded with the tire inflation pressure; (ii) the axisymmetric model was revolved to create full 3-D model; and (iii) free-rolling analysis was performed. It should be noted that during the static phase, frictionless interaction between tire and road was assumed. The Coulomb friction model was applied when performing free-rolling analysis.

4. Numerical analysis matrix

The numerical analysis matrix was designed to investigate the effect of typical truck tire operating conditions on rolling resistance. Three values of load, tire inflation pressure, temperature and speed were combined to create 81 analysis cases. The tire inflation pressure ranged from 552 kPa, which represents under-inflated tire, to 758 kPa, which is slightly higher than recommended inflation pressure for most truck tires. The lowest and highest load values were 26.2 to 44.4 kN. It must be noted that for a semi-truck with four axles, the typical load is 37.8 kN on one tire. Travelling speeds were 8, 65 and 115 km/h, which represent the range of truck speeds, including low speed in urban areas and high speed on highways. Finally, tire temperature was assumed constant and equal to 25, 45 and 65°C. Table 1 summarises the values of the variables considered. The effect of temperature on tire inflation pressure was omitted.

Table 1. Values of load, inflation pressure, speed and temperature considered.

Load	Pressure	Speed	Temperature
(kN)	(kPa)	(km/h)	(°C)
P1 = 26.6	S1 = 552	V1 = 8	T1 = 25
P2 = 35.5	S2 = 690	V2 = 65	T2 = 45
P3 = 44.4	S3 = 758	V3 = 115	T3 = 65

5. Rolling resistance from dissipated energy and longitudinal reaction force

Based on the FE model described, two methodologies can be followed to calculate rolling resistance: The energy dissipated by the tire divided by the distance travelled in one revolution (RR_e), and the reaction force in the travelling direction, (RR_f), which is the mechanical manifestation of dissipated energy. The coefficient of rolling resistance C_{rr} is commonly used as an indicator of rolling resistance per applied load, and it is believed to characterise the rolling resistance of a tire under various applied loads. Pillai and Fielding-Russell theoretically linked rolling resistance and energy dissipation assuming constant contact area and uniform distribution of tire-pavement contact stresses (Pillai and Fielding-Russell 1992). It was proved that:

$$RR = h\frac{P\delta b}{A_c}$$

(1)

where

$RR = \text{rolling resistance}$

$h =$ ratio of energy lost to the total energy input
$P =$ applied load
$\delta =$ tire deflection
$A_c =$ contact area
$b =$ width of contact area.

In other words:

$$C_{rr} = \frac{RR}{P} = h\frac{\delta b}{A_c}$$

(2)

From Equation (2), it can be concluded that, for the coefficient of rolling resistance to characterise the energy dissipated by the tire, the term $\delta b/A_c$ needs to be constant. The assumption was verified for the variables summarised in Table 1 using the developed FE model. Figure 4 presents the variation of $\delta b/A_c$ with load, tire inflation pressure, speed and temperature. Each mark shape represents a different temperature (circle, $T = 25$℃; triangle, $T = 45$℃; and square, $T = 65$℃). The negligible effect of V was observed. In addition, a variation between 0.332 and 0.286 in the vertical axis and a coefficient of variation of 3.5% was also seen, thus confirming that the assumption that $\delta b/A_c$ being constant is acceptable for the studied tire. Consequently, rolling resistance based on equilibrium RR_f was adopted as indicator of the energy dissipation in this study.

Figure 4. Variation of $\delta b/A_c$ with variables considered.

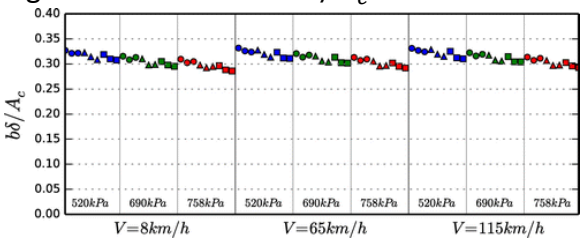

The rolling resistance was calculated using Schuring (1980):

$$RR_f = \frac{T\omega}{V} - F_x$$

(3)

where

$RR =$ rolling resistance
$V =$ rolling speed of the tire
$\omega =$ angular velocity
$F_x =$ resulting longitudinal force.

6. Influence of operating conditions on the baseline rolling resistance

FE simulation results were analysed to evaluate rolling resistance in the tire as a result of different operating conditions. Rolling resistance values based on the equilibrium and Equation (3) were

retrieved for each operating condition. Figure 5 shows the effect of tire inflation pressure and load on the RR_f for extreme T and V. The horizontal axis represents the tire inflation pressure, while the vertical is the RR_f. All computed RR_f are summarised in Table 2.

Figure 5. Variation of rolling resistance with load, temperature, speed and tire inflation pressure.

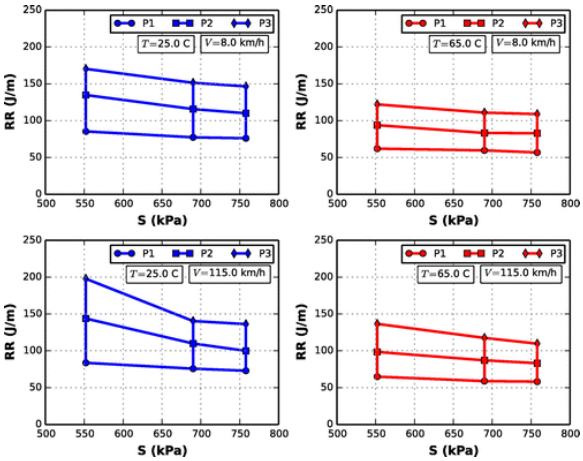

RR_f decreased with the change of S for all magnitudes of the applied load. The highest and lowest diminution of rolling resistance were 8.3 and 31.1%, respectively. When $V = 115$ km/h and $T = 25$°C, RR_f decreased 31.1% when changing the tire inflation pressure from 552 to 756 kPa at $P = 44.4$ kN. The reduction could be as low as 8.3%, as in the case $P = 26.6$ kN, $T = 65$°C, and $V = 8$ km/h, where RR_f changed from 62.0 N when $S = 552$ kPa to 56.8 N when $S = 758$ kPa. The effect of tire inflation pressure was smaller at low load because the load caused the deformation in the tire to increase, thus counterbalancing the stiffening effect of S.

By tracking the rate of change of RR_f with respect to P, it was concluded that, once all other variables are unchanged, rolling resistance varies almost linearly with load. For example, the ratio between RR_f when $P = 35.5$ kN and $P = 26.6$ kN is 1.43, which is very close to 1.35, the ratio of RR_f when $P = 44.4$ kN and $P = 35.5$. These values correspond to $S = 758$ kPa, $V = 65$ km/h and $T = 65$°C (the ratio instead of constant slope was used as criteria to check linearity because the load increment was constant, 8.9 kN).

Table 2. Rolling resistance for variables in numerical analysis matrix.

		8 km/h			65 km/h			115 km/h		
		S1	S2	S3	S1	S2	S3	S1	S2	S3
77°F	P1	85.39	77.36	76.07	84.98	71.19	68.90	83.69	75.75	72.96
	P2	134.79	115.71	110.01	131.87	111.95	104.45	143.84	109.93	99.94
	P3	170.28	151.39	146.52	189.26	152.61	148.74	197.81	140.40	136.27
113°F	P1	65.03	59.37	58.52	82.07	74.93	73.89	85.07	77.30	76.11
	P2	99.12	87.04	83.78	112.48	109.98	104.73	128.41	114.24	109.41
	P3	135.73	119.82	113.62	165.56	146.27	140.20	173.94	153.45	146.47
149°F	P1	61.99	59.61	56.81	63.94	58.51	57.90	64.91	58.88	58.17
	P2	93.87	83.27	82.66	98.25	86.31	82.82	98.51	87.08	83.22
	P3	122.09	110.89	108.93	134.29	121.01	112.11	136.59	117.50	109.72

It is clearly shown that temperature has a significant effect on rolling resistance. First, as the temperature increased, the slope of the lines in Figure 5 slightly reduced, to the point of becoming almost horizontal when $T = 65$℃. When $P = 44.4$ kN, $T = 25$℃, and $V = 115$ km/h, RR_f reduced 61.5 N between $S = 520$ and 758 kPa. When the temperature changed to 65℃, the reduction decreased to 26.9 N for the same tire inflation pressures. This behaviour is caused by the temperature effect on the tire stiffness. Second, the separation between the lines of equal load decreased as temperature increased, indicating a diminishing effect of load with temperature increment. The case $S = 552$ kPa, $V = 65$ km/h and $T = 25$℃ showed an increment of 57.4 N in rolling resistance after increasing the load from 35.5 to 44.4 kN. The increment for the same V and S fell to 36.0 N if the temperature switched to $T = 65$℃.

Rubber components are viscoelastic materials, which means its modulus depends on the temperature and loading rate. As the temperature increased, the tire stiffness decreased to the point where the stiffening effect of increasing tire inflation pressure became insignificant. Because speed is closely related to the loading rate, the loading rate augmented with the increase in speed, the tire was stiffer, the deformation reduced and the rolling resistance diminished. However, one should not expect a monotonically increasing or decreasing trend with dissipated energy as it is derived from stresses and a viscous components of the viscoelastic strains. As the loading rate increases or temperature decreases, stresses may augment in the rubber, accompanied with a reduction in the viscous part of strains, which may result in higher dissipated energy as long as the reduction in viscous strains can be compensated by a gain in stresses.

The effect of temperature is not uniform across the range of analysed values. In particular, for the loading condition $P = 44.4$ kN, $S = 690$ kPa, and slowest rolling speed, RR_f decreased 20.9% from 151.4 to 119.8 N if the temperature was changed from $T = 25$ to 45℃. Conversely, 7.5% reduction was noticed when the temperature changed from $T = 45$ to 65℃. Speed has a diminishing influence on the effect of increasing the temperature from the lowest values. If the same loading condition is analysed, but for $V = 65$ km/h, the reduction from the lowest to medium temperature will not be 20.9%, but 6.3%.

Speed and temperature effects on RR_f were opposite. Thus, increasing the travelling speed caused an increase in rolling resistance. The influence was higher when changing from $V = 8$ to $V = 65$ km/h than from $V = 65$ to $V = 115$ km/h. The average increment of RR_f after increasing speed from lowest to medium speed was 24.4%, while it was 4.3% from medium to highest speed. These averages include all values of load, tire inflation pressure, at $T = 45$℃. It is worth to mention that the effect of speed was higher at the intermediate temperature.

Finally, it should be mentioned that the coefficient of rolling resistance calculated using Equation (2), varied between 0.0045 and 0.0021. The range is close to the one reported in some literature for the wide-base tire technology (Michelin of Americas 2003).

7. Regression analysis

A predictive equation was developed using the regression analysis applied to the rolling resistance results obtained. SAE J2452 is based on load, tire inflation pressure and speed, but it does not consider temperature. To address this drawback, a temperature-dependent factor was included in the SAE

equation. The following form of rolling resistance is proposed to capture temperature and speed dependency:

$$RR_e = k\frac{S^a P^\beta}{\sqrt{T}}(a + bV + cV^2)$$

(4)

Where k, α, β, a, b and c are regression parameters. Using nonlinear least square method, the fitting parameters were found as $k = 0.2740$, $\alpha = -0.6392$, $\beta = 1.3618$, $a = 10.68 \times 10^{-3}$, $b = 26.23 \times 10^{-6}$ and $c = -129.1 \times 10^{-9}$, so the final equation becomes:

$$RR = 2.740 \times 10^{-4}\frac{S^{-0.6392}P^{1.3618}}{\sqrt{T}} \times \left[10.68 + 26.23\left(\frac{V}{10^3}\right) - 129.1\left(\frac{V}{10^3}\right)^2\right]$$

(5)

Figure 6 compares the rolling resistance from the FE model and Equation (5). As can be seen, a coefficient of correlation of $R^2 = 0.946$ was obtained, which is very good considering that the range of values of the considered variables covered typical operating conditions of truck tires.

Figure 6. Comparison between rolling resistance from FE model and using Equation (5).

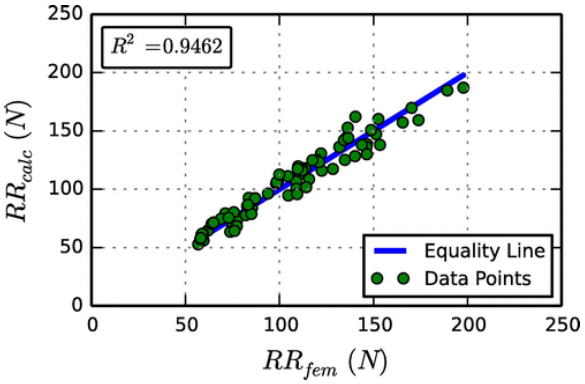

8. Energy per tire component

As previously shown in Figure 1, four viscoelastic rubber components were considered: tread, subtread, shoulder and sidewall. Since the material properties and volume of each rubber element are different, their contribution to the internal energy of the tire, IE_{tire}, varied. The variation of IE_{tire} and its components with respect to P, S, V and T is presented in Figure 7. In the figure, a combination of load and tire inflation pressure consists of three bars, each representing a speed in ascending order.

Figure 7. Internal energy in tire's rubber components. (a) $T = 25$°C, (b) $T = 45$°C, and (c) $T = 65$°C.

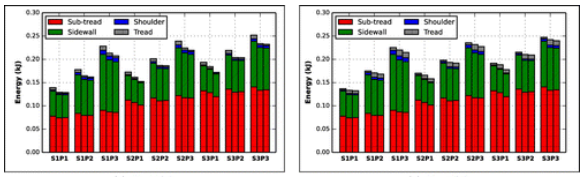

(a) T=25°C.

(b) T=45°C.

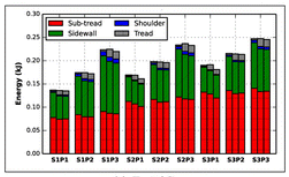

(c) T=65°C.

The subtread and sidewall had the highest contribution to IE_{tire}. The ratio of the internal energy in the subtread, IE_{st}, to IE_{tire} varied between 38.8 and 69.7%, while the one in the sidewall, IE_{sw}, was higher than 26.5% but smaller than 52.5%. In addition, the sidewall's internal energy was higher than the one in the subtread only when the tire was subjected to the lowest tire inflation pressure and highest load. For $T2$ and $T3$, the tread represented higher internal energy than the shoulder, not only in magnitude, but also in percentage of the total energy in the tire. However, the tread and the shoulder were not as relevant for IE_{tire}; the highest ratio between each of the two elements and IE_{tire} was 0.078 and 0.042, respectively.

At the highest temperature, speed did not greatly affect total energy. The highest change after increasing the speed from 8 to 115 km/h when $T = 65℃$ was 5.0% . On the other hand, for the lowest temperature, the reduction reached 11.7%. Furthermore, the applied load greatly affected the internal energy in the sidewall IE_{sw}. The increment, which was linear, varied between 1.8 and 2.2 times the value of the lowest load. The change was higher at low tire inflation pressure.

Finally, the trend of the tire component's contribution to IE_{tire} and the corresponding percentage was similar, except for the subtread. For this tire material, the total contribution increased with P and S, but the ratio between IE_{st} and IE_{tire} decreased as the tire inflation pressure augmented.

9. Conclusions

FE modelling of a truck tire was developed to calculate rolling resistance as a function of different operating conditions, including temperature, speed, load and tire inflation pressure. The complex nature of the tire was captured using a 3-D FE tire model with realistic geometric details. Material characteristics were obtained from relevant experiments. Incompressible visco-hyperelastic constitutive relationship for rubber materials was used to calculate the rolling resistance.

The methods that are based on the reaction force along the travelling direction and coefficient of rolling resistance as indicators of tire fuel efficiency were found to be satisfactory in capturing consistent trends with changing speeds and temperatures. Therefore, an equilibrium-based rolling resistance calculation method was adopted in this study. The effect of tire inflation pressure, travelling speed, applied load and tire temperature was successfully quantified. It was found that temperature and load had the highest effect on rolling resistance, while speed and tire inflation pressure did not modify rolling resistance as significantly. A predictive equation was developed based on the results of the FE simulations. The SAE J2452 expression for rolling resistance was modified to include the

temperature effect. Finally, the contribution of each rubber component to the tire's internal energy was quantified, showing a more relevant role of subtread and sidewall.

This research is the first step to quantify the effect of pavement structure and tire-pavement interaction on fuel consumption and life-cycle assessment of road infrastructure.

Additional information

Funding

This work used the Extreme Science and Engineering Discovery Environment (XSEDE), which is supported by National Science Foundation [grant number ACI-1053575].

Notes

No potential conflict of interest was reported by the authors.

References

1. Ang-Olson, J. and Schroeer, W., 2002. Energy efficiency strategies for freight trucking: potential impact on fuel use and greenhouse gas emissions. *Transportation Research Record*, 1, 11–18.
2. Bureau of Transportation Statistics, 2013. *National transportation statistics. Technical report*. Washington, DC: Department of Transportation.
3. Chatti, K. and Zaabar, I., 2012. *Estimating the effects of pavement condition on vehicle operating costs. Technical report*. East Lansing, MI: Michigan State University.
4. Clark, S.K., 1978. Rolling resistance of pneumatic tires. *Tire Science and Technology*, 6 (3), 163–175.
5. Danielson, K.T. and Noor, A.K., 1997. Finite elements developed in cylindrical coordinates for three-dimensional tire analysis. *Tire Science and Technology*, 25 (1), 2–28.
6. Ebbott, T., *et al.*, 1999. Tire temperature and rolling resistance prediction with finite element analysis. *Tire Science and Technology*, 27 (1), 2–21.
7. Franzese, O., Knee, H.E.B., and Slezak, L., 2010. Effect of wide-based single tires on fuel efficiency of class 8 combination trucks. *Transportation Research Record: Journal of the Transportation Research Board*, 2191 (1), 1–7.
8. GENIVAR, 2005. *Economic study: Use of supersingle tires by heavy vehicles operating in Qubec. Technical report*. Montreal, QC: GENIVAR Consulting Group.
9. Grover, P.S., 1998. Modeling of rolling resistance test data. *SAE Technical Paper Series*, 980251.
10. Helnwein, P., *et al.*, 1993. A new 3-D finite element model for cord-reinforced rubber composites application to analysis of automobile tires. *Finite Elements in Analysis and Design*, 14 (1), 1–16.
11. Hernandez, J., Al-Qadi, I., and De Beer, M., 2013. Impact of tire loading and tire pressure on measured 3D contact stresses. In: *Airfield and Highway Pavement 2013: Sustainable and Efficient Pavements*, Los Angeles, CA: American Society of Civil Engineers, 551–560.
12. Hernandez, J.A. and Al-Qadi, I.L., 2015. Hyperelastic modeling of widebase tire and prediction of its contact stresses. *Journal of Engineering Mechanics*, p. 04015084.
13. Kennedy, R.H., 2003. Experiences with cylindrical elements in tire modeling. In: *ABAQUS Users' Conference*, Simulia, 15.

14. Laclair, T.J. and Russell, T., 2005. Modeling of fuel consumption for heavy-duty trucks and the impact of tire rolling resistance. *SAE Technical Paper Series*, 2005-01-3550.
15. Lou, A.Y.C., 1978. Relationship of tire rolling resistance to the viscoelastic properties of the tread rubber. *Tire Science and Technology*, 6 (3), 176–188.
16. Mammetti, M., *et al.*, 2013. The influence of rolling resistance on fuel consumption in heavy-duty vehicles. *SAE Technical Paper Series*. 2013-01-1343.
17. Michelin of Americas, 2003. *The tyre rolling resistance and fuel savings. Technical report*. Michelin of Americas.
18. Muster, T., 2000. *Fuel savings potential and costs considerations for US class 8 heavy duty trucks through resistance reductions and improved propulsion technologies until 2020. Technical report*. Cambridge, MA: Massachusetts Institute of Technology.
19. Nielsen, L. and Sandberg, T., 2002. A new model for rolling resistance of pneumatic tires. *SAE Technical Paper Series*, 2002-01-1200.
20. Nylund, N.O., 2006. *Fuel savings for heavy duty vehicles. Technical report*. Finland: VTT.
21. Pillai, P.S., 1995. Total tire energy loss comparison by the whole tire hysteresis and the rolling resistance methods. *Tire Science and Technology*, 23 (4), 256–265.
22. Pillai, P.S. and Fielding-Russell, G.S., 1992. The rolling resistance from whole-tire hysteresis ration. *Rubber Chemistry Technology*, 65, 444–452.
23. Schuring, D.J., 1980. The rolling loss of pneumatic tires. *Rubber Chemistry and Technology*, 53 (3), 600–727.
24. Schuring, D.J., 1994. Effect of tire rolling loss on vehicle fuel consumption. *Tire Science and Technology*, 22 (3), 148–161.
25. Schuring, D.J. and Redfield, J.S., 1982. Effect of tire rolling loss on fuel consumption of trucks. *SAE Technical Paper Series*, 821267.
26. Shida, Z., *et al.*, 1999. A rolling resistance simulation of tires using static finite element analysis. *Tire Science and Technology*, 27 (2), 84–105.
27. Society of Automotive Engineers, 1999. Stepwise coastdown methodology for measuring tire rolling resistance. *SAE Standards*.
28. Society of Automotive Engineers, 2006. Rolling resistance measurement procedure for passenger car, light truck, and highway truck and bus tires. *SAE Standards*.
29. Terziyski, J. and Kennedy, R., 2009. Accuracy, sensitivity, and correlation of FEA-computed coastdown rolling resistance. *Tire Science and Technology*, 37, 4–31.
30. The White House, 2014. *Improving the fuel efficiency of American trucks. Technical report*. The White House
31. Walter, J.D. and Conant, F.S., 1974. Energy losses in tires. *Tire Science and Technology*, 2 (4), 235–260.
32. Wen, B., Rogerson, G., and Hartke, A., 2014. Correlation analysis of rolling resistance test results from SAE J1269 and J2452. *SAE Technical Paper Series*. 2014-01-0066.